Proceedings World Geothermal Congress 2010
Bali, Indonesia, 25-29 April 2010

The Nature of Reservoir Fracture Heterogeneity: II -- Rapid Interwell Connectivity Simulation for Reservoir-Scale Structure Modeling

Peter C Leary and Peter E Malin

Institute of Earth Science and Engineering, University of Auckland, 58 Symonds Street, Auckland 1142, New Zealand

p.leary@auckland.ac.nz; p.malin@auckland.ac.nz

Keywords: fracture heterogeneity, percolation flow, numerical reservoir flow modeling

ABSTRACT

Reservoir well-log and well-core data show that geofluids tend to flow along microfracture-related percolation pathways. These pathways arise from scale-independent, long-range spatial correlation processes at scale lengths from mm (grain-scale) to km (reservoir-scale). Percolation pathway spatial fluctuation power $S(k)$ scales inversely with spatial frequency k, $S(k) \sim 1/k$. As such the pathways are inherently spatially erratic and unpredictable at all scale lengths. Thus no valid statistical means relates well-scale sample data to reservoir-scale flow structures. It follows that standard flow models based on geometrically-regular geological and/or fracture formations derived from well-scale reservoir samples cannot accurately predict large-scale flow patterns. Flow predictions must, instead, be based on *in situ* reservoir flow data at the scale for which the flow is actually taking place.

For reservoir-scale modeling, interwell connectivity is a logical basis for defining flow structures that cannot be predicted from borehole-scale sampling. A new physical/computational model of *in situ* fracture systems allows interwell connectivity field data to be built into adequate reservoir-scale flow models. Flow simulation in the physically-based fracture-heterogeneous model systems is efficiently computed by standard finite-element solvers. In the new flow-computational scheme for fracture-heterogeneous reservoirs, numerical grids of dimension 32 x 64 x 64 to 64 x 128 x 128 are used to compute inter-well connectivity. Interwell connectivity systematics can be expressed in relation to interwell flow in a uniform-permeability reservoir. Flow model data can distinguish between three spatial fracture density scaling regimes:

(i) $1/k^0$ (uncorrelated, white or Gaussian fluctuation noise),

(ii) $1/k^1$ ($1/f$-noise fluctuations), and

(iii) $1/k^2$ (Brownian noise equivalent to block-like flow spatial fluctuations).

Fracture density scaling regimes (i) and (iii) are often assumed for reservoir heterogeneity but are not validated by observation. Fracture density scaling regime (ii) is, instead, almost universally observed in well-log data. Whole-reservoir flow structures can thus be inferred from observing interwell connectivity deviations from the uniform permeability case. Interwell connectivity data quantified by the $1/k$-scaling model physically links flow to individual well pressure, temperature, and solute concentration data. The physical basis for *in situ* flow modeling also provides a first-order geomechanics model for conducting massive fracturing of lower permeability rock volumes to boost geothermal well production, and allows related geophysical field data (seismic, micro-earthquake, magnetotelluric) to be quantitatively interpreted in terms of fracture-heterogeneous flow structures.

1. INTRODUCTION: DETECTING FLOW HETEROGENEITY IN HYDROCARBON AND GEOTHERMAL RESERVOIRS

A long-term symptom of reservoir flow heterogeneity has been the persistent failure of flow models to predict the flow behavior of individual wells. Standard reservoir models typically fail to predict either hydrocarbon or geothermal well productivity, the onset of water cut in hydrocarbon production wells, or well injectivity for waste water in hydrocarbon and geothermal reservoirs. Likewise, standard reservoir models rarely accurately predict well-to-well connectivity in either hydrocarbon or geothermal reservoirs, nor model bypassed reserves in hydrocarbon reservoirs. Further afield, crustal reservoir models have failed to deal convincingly with risk assessment in nuclear waste site validation.

To address reservoir model uncertainty in hydrocarbon reservoirs it is now commonplace in the oil and gas industry to conduct time-lapse seismic imaging of reservoir formations to directly measure the spatially erratic distribution of *in situ* porosity and permeability revealed by lighter or compressible oil/gas replacement by heavier or less compressible water. In tight gas sands, produced gas leads to reduced formation fracture porosity that changes formation velocity; the changes can be imaged by precision time-lapse seismometry to spatially locate the more productive fracture-dense parts of the reservoir volume for infill drilling (Leary and Walter, 2008).

Mapping fluid substitution/evacuation processes is not, however, a feasible tactic for mapping hydrothermal reservoir flow system heterogeneity. High temperatures, steady-state circulation of working fluids, and insignificant physical difference between hotter and colder groundwater require a different form of operator intervention to perturb the reservoir. One such intervention is the imposing of massive hydrofractures on the reservoir rock. Such fracture stimulation tactics are fundamental to tight gas production and to engineered geothermal systems (EGS) in tight metamorphic/igneous rock. In the more permeable hydrothermal systems discussed here, operator intervention typically comes from routine changes in the otherwise steady buoyancy flow conditions recorded at closely spaced production and observation wells. Such variable flow data are a natural candidate for observing the presence or absence of pair-wise or group interwell connectivity (Horne and Szucs, 2007; Horne, 2008). If massive fracture stimulation of lower permeability rock in hydrothermal reservoirs proves to be an effective way to counter the inability to reservoir models to locate high permeability volumes at depth, the fracture-borne flow simulations

discussed here may useful in planning and monitoring such measures.

2. NUMERICAL REALIZATION OF RESERVOIR HETEROGENEITY CONSISTENT WITH WELL-LOG AND WELL-CORE DATA

A systematic well-log and well-core phenomenology forms the basis for the numerical flow simulation discussed in this paper. Our companion paper (Leary and Malin, 2010) reviews the evidence for *in situ* reservoir properties being influenced or controlled by spatially fluctuating number density $\nu(x,y,z)$ of grain-scale fractures. The following properties are observed to apply to a wide range of crustal reservoirs:

- Spatial fluctuations occur systematically from grain-scale to reservoir-scale in accordance with well-log power-spectra of form $S(k) \sim 1/k$ with spatial frequency k ranging over five decades, $\sim 1/\text{km} < k < \sim 10^5$ /km;
- Reservoir permeability is controlled by reservoir porosity through grain-scale percolation connectivity fluctuation relation $\delta\nu \approx \delta\log(\nu!)$ in accordance with well-core porosity/permeability (poroperm) fluctuation relation $\delta\varphi \approx \delta\log(\kappa)$.

These properties can be consistently interpreted in terms of scale-independent interactions between crustal volumes of spatially fluctuating numerical grain-scale-fracture density $\nu(x,y,z)$. It is straightforward to generate numerical volumes that have the intrinsic spatial fluctuation character of *in situ* physical properties of crustal reservoirs expressed through number density (Turcotte, 1992; Leary, 2002). With this numerical realization of *in situ* fracture fluctuation phenomenology, geofluid flow in fracture-heterogeneous media can be computed using finite element solvers for the spatially fluctuating pressure field $P(x,y,z)$ of Darcy's diffusion law (Voss and Provost, 2008; Leary and Walter, 2008; Regenauer-Lieb et al., 2009):

$$\partial_t P = \underline{\nabla} \bullet \left(\kappa(x,y,z)\underline{\nabla} P\right)$$

Finite-element solutions to fluid flow in and out of elementary digital volumes or cells are robust against spatial variations in the porosity and permeability of cells. The fact that these property spatial variations occur at all scale lengths throughout numerical medium has no effect on the speed or stability of the flow computations. It is straightforward to run simulations with 64 x 128 x 128 = 2^6 x 2^7 x 2^7 cells on workstations to give six octaves of vertical fluctuation power and seven octaves of lateral fluctuation power, equivalent to factors 8 and 11, respectively, in porosity amplitude fluctuations equivalent to several orders of magnitude in permeability fluctuations over almost 3 decades of scale length.

The flow simulations described here focus on fracture heterogeneity flow control. Accordingly, flow is restricted to a single phase, with heat transport and/or the steam phase left to subsequent simulations. Geological structural complexity is also omitted. Vertical buoyancy is the main flow driver, with spatial fluctuations in horizontal flow providing the main signal diagnostic of *in situ* fracture heterogeneity and well-connectivity.

We model three generic forms of broadband heterogeneity controlled by fracture-structure interconnectedness within reservoir flow systems. If two wells are within the same fracture-permeability structure, they are likely to show interwell connectivity of a given amplitude and time-lag. If, on the other hand, two wells belong to different fracture-permeability structures, they are not likely to show interwell connectivity of significant amplitude or within an easily interpreted time-lag.

Given the plausible range of well-well connectedness, it is logical to distinguish between flow models in which the generic physical nature of reservoir flow heterogeneity fundamentally accords with flow heterogeneity exhibited by well-log fluctuation systematics versus flow models which are discordant with well-log data. In both cases, we assume a percolation flow mechanics based on clastic reservoir well-core fluctuation systematics. Our modeling tactic is to keep as close as possible to a broadly accurate generic physical account of the *in situ* geofluid flow process rather than to introduce a narrow range of arbitrary flow model structures and or assumptions.

Our limited repertoire of heterogeneity models nonetheless precisely encompasses the two extremes of rock heterogeneity modeling. One extreme, models rock heterogeneity as spatially uncorrelated or white/Gaussian noise with fluctuation power spectra $S(k) \sim 1/k^0$. This is the default assumption usually imposed by modelers on the physical nature of geological media. The extreme of spatial heterogeneity modeling effectively imposes a strong degree of spatial correlation via the Brownian noise spectrum $S(k) \sim 1/k^2$. Brownian noise can be thought of as simulating crustal blocks/volumes separated by interfaces, thus inducing a high degree of long-wavelength spatial correlation compared with short-wavelength spatial correlation. Brownian spectra are characteristic of media in which the dominant nature of the medium is abrupt physical property changes at geological interfaces. These two model extremes of spatial correlation for geological media contrast with the intermediate case of our generic reservoir models, where spatial correlations are controlled by the '1/*f* noise' spectrum, $S(k) \sim 1/k$. This degree of model spatial correlation is conspicuously different from both of the 'geologically oriented' models and agrees with *in situ* fluctuation data. As such it is the main focus of our flow simulations.

Figures 1-3 illustrate the degree of spatial correlation given by $S(k) \sim 1/k^0$, $S(k) \sim 1/k^1$, and $S(k) \sim 1/k^2$, respectively.

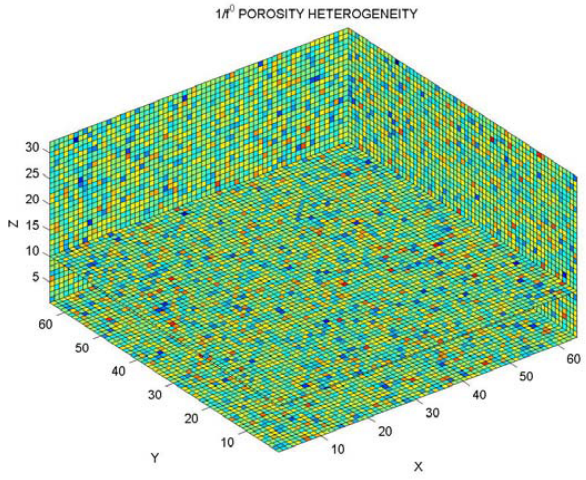

Figure 1: 3D uncorrelated or white/Gaussian spatial noise porosity fluctuations; well-logs through the volume have power-law spectra $S(k) \sim 1/k^0$.

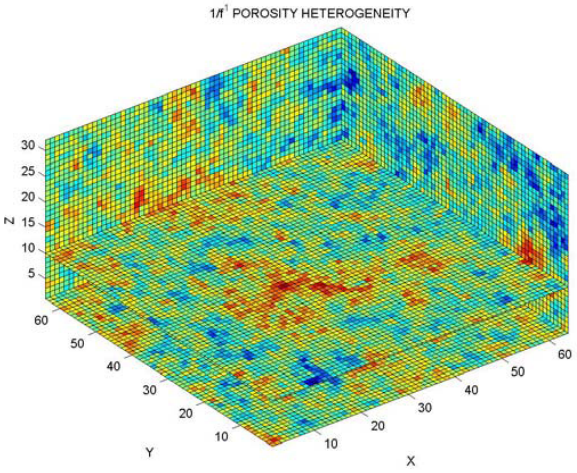

Figure 2: 3D 1/*f*–noise spatial porosity fluctuations consistent with *in situ* well-log spectra $S(k) \sim 1/k^1$.

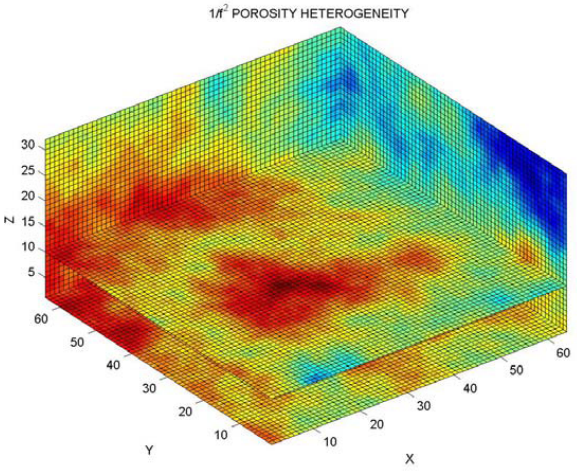

Figure 3: 3D Brownian–noise spatial porosity fluctuations with spectra scaling as $S(k) \sim 1/k^2$; this distribution shows that strong spatial correlation leads to block-like partition of geophysical properties.

Figures 1-3 together with Figure 4 outline the main features of our flow simulations. Flow takes place in a data cube of node dimension 64 x 64 x 32 (node dimension 128 x 128 x 64 is feasible but slower). The data cube is uniform except for spatially heterogeneous distributions of porosity and permeability. Porosity distributions are determined by a set of node numbers $\varphi_0 < \varphi(i,j,k) < \varphi_1$. Permeability is derived from the mean of eight node porosities surrounding each permeability point; permeability is assigned according to the *in situ* well-core fluctuation relation $\delta\varphi \approx \delta\log(\kappa)$.

The data cube is assumed to be saturated with water initially in hydrostatic equilibrium. The sides of the data cube are held at constant pressure boundary conditions to permit fluid flowing in the interior of the data cube to force water out of the computational volume if called to do so by source conditions imposed within the data cube interior. The data cube bottom and top are maintained at constant pressure (zero at the top, hydrostatic at the bottom).

Flow is initiated by fluid pressure at an interior point. Fluid motion is dominantly vertical through buoyancy forces but horizontal flow occurs due to lateral pressure in the vertical column above the injection point. The lateral flow boundary conditions effectively simulate an unbounded flow medium surrounding the simulation volume.

Figure 4 calibrates flow simulation displays in Figures 5 to 8 for lateral flow for a uniform poroperm medium. The color of each display point denotes the magnitude of horizontal flow velocity just above the pressure injection point. Dark blue denotes low velocities and brown/red denote high velocities. In Figure 4 the horizontal velocity field is azimuthally uniform and falls off as a function of radially diminishing differential pressure. As expected for a uniform medium, flow is directly controlled by the pressure field at the source point.

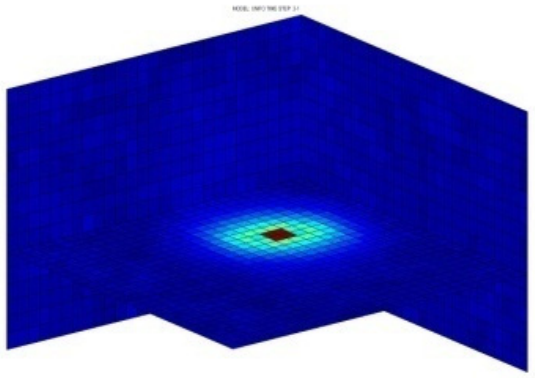

Figure 4: Snapshot of flow computation numerical volume for uniform poroperm medium. A pressure source at centre of source plane induces buoyancy flow coupled to horizontal flow denoted by color variation: high horizontal flow (brown) grades to low horizontal flow (dark blue) with increasing distance from the source.

Figures 5-8 show Figure 4 flow simulation conditions in the presence of poroperm heterogeneity. The figures show the time-step horizontal flow evolution for the different degrees of spatial correlation illustrated in Figures 1-3. Model heterogeneities have the same mean porosity and permeability as the Figure 4 uniform medium, with each porosity distribution having the same magnitude of fluctuation power. The only difference between the three flow simulations is the degree of spatial correlation of porosity and permeability heterogeneity.

The Figure 5-8 time-sequence is normalized to an initial time at which the numerical flow regime has been established. Unlike Figure 4 for uniform media, each of Figures 5-8 has significant flow differences at many points surrounding the source point. In each case lateral flow occurs without clear spatial connection to the source point but the details of this disconnection vary in time and space with heterogeneity type. In the spatially uncorrelated ($S(k) \sim 1/k^0$) heterogeneity medium, flow velocity is distributed erratically about the source point and evolves slowly as the buoyancy field drives fluids laterally away from the central buoyancy column. A similar temporal progression occurs for the strongly correlated Brownian ($S(k) \sim 1/k^2$) heterogeneity field, but the flow is spatially constrained to a coherent locus as if there were a geological partition to the reservoir medium; Figure 3 shows that flow is controlled by the spatial distribution poroperm properties. The intermediate 1/*f*-noise spatial correlation heterogeneity ($S(k) \sim 1/k^1$) proves more complex. The flow history is uneven as fluid flowing away from the central column reaches irregular and erratic spatially-correlated flow channels that require time to equilibrate.

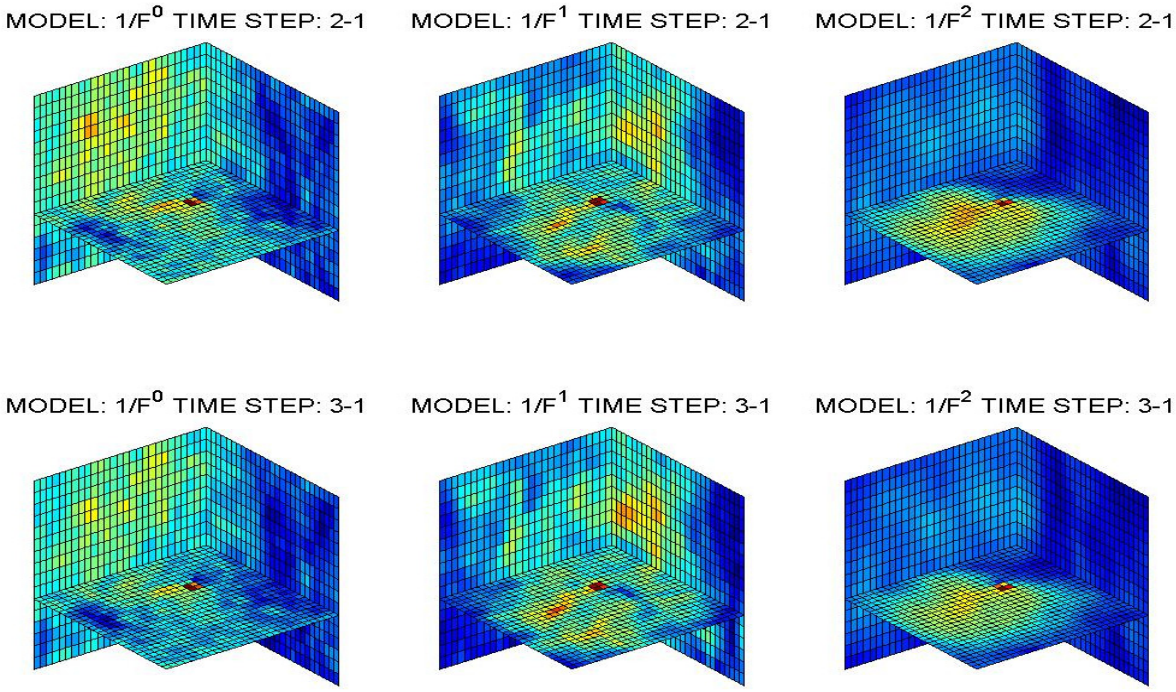

Figure 5: Snapshots for time-steps 2 and 3 showing horizontal flow magnitude in numerical simulation volume for three poroperm media: (left) uncorrelated spatial noise, $S(k) \sim 1/k^0$; (centre) 1/*f*-noise, $S(k) \sim 1/k^1$; (right) Brownian spatial noise, $S(k) \sim 1/k^2$. A pressure source at centre of source plane induces buoyancy flow coupled to horizontal flow denoted by color variation: high horizontal flow (brown) grades to low horizontal flow (dark blue). For Brownian spatial correlation, flow is largely confined to the high permeability volume seen in Figure 3. For Gaussian and 1/*f*-noise spatial correlation, flow is more widely disseminated, with flow in the 1/*f*-noise poroperm distribution influence by the spatial distribution seen in Figure 2.

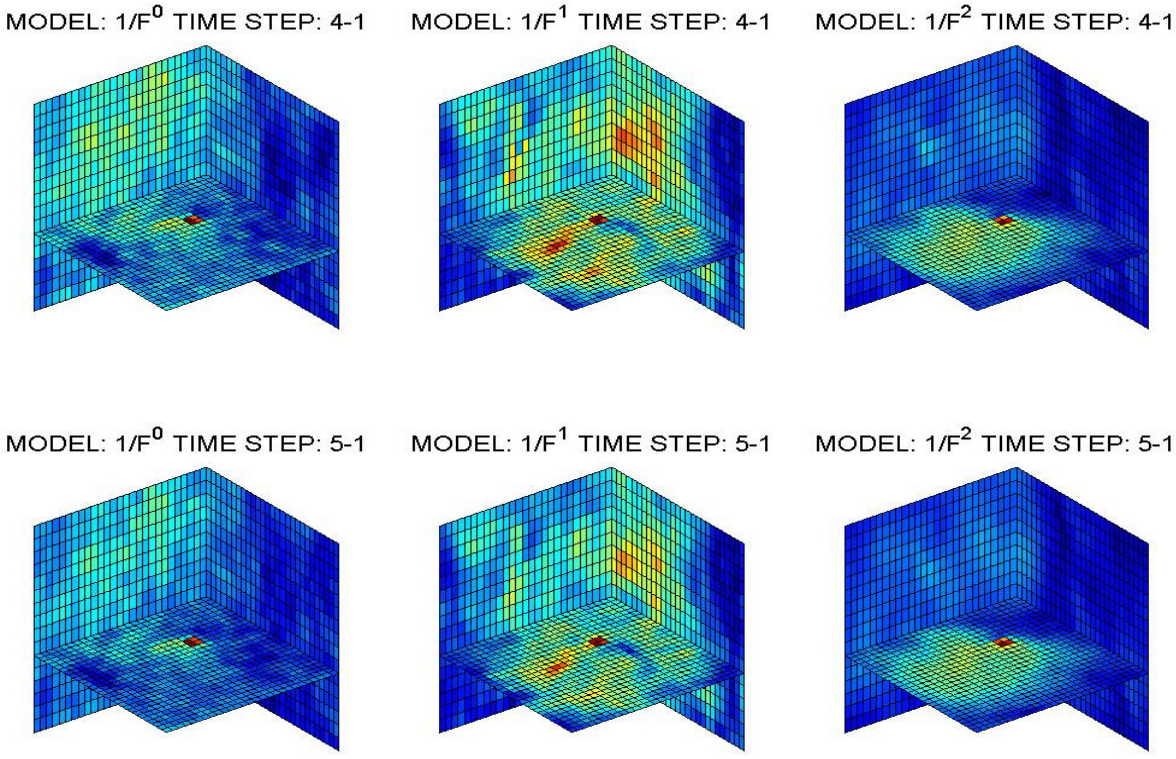

Figure 6: Snapshots for time-steps 4 and 5 of flow simulation described in Figure 5; flow in the uncorrelated spatial noise medium (left) is diminishing with time while flow in the 1/*f*-noise medium (centre) is increasing with time as the complex spatially correlated percolation pathways conduct fluids in irregular pathways.

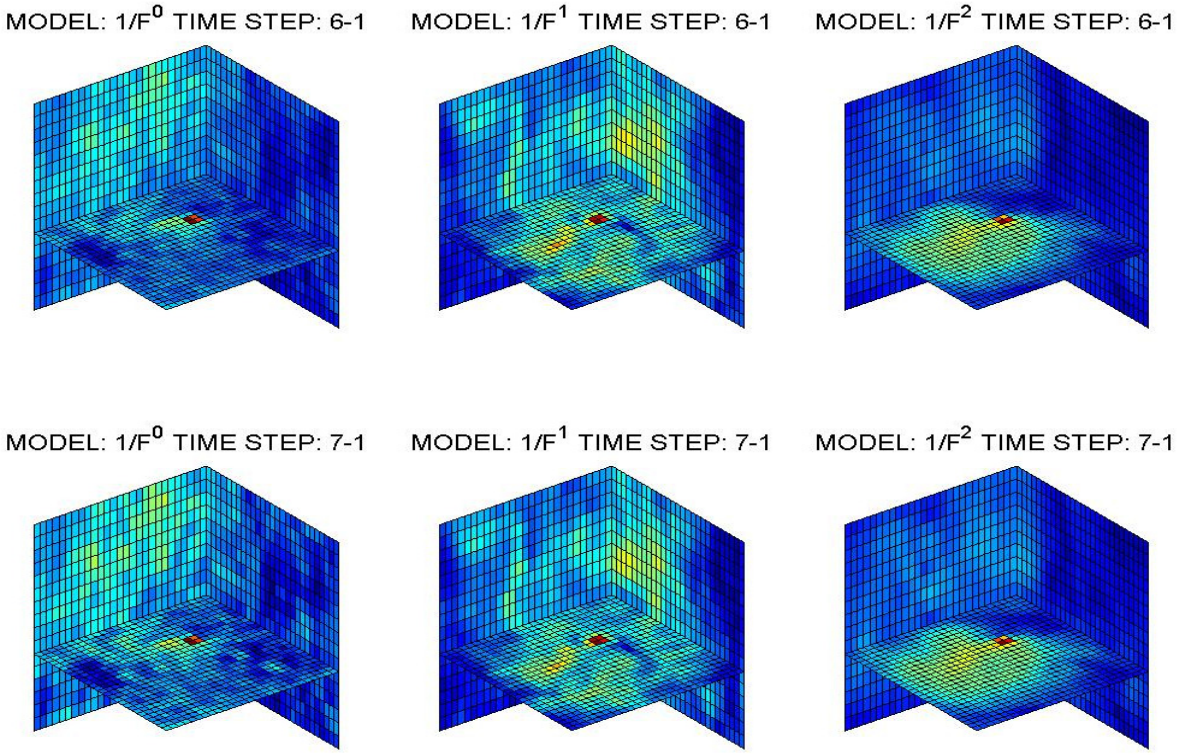

Figure 7: Snapshots for time-steps 6 and 7 of flow simulation described in Figure 5; flow in the 1/*f*-noise medium (centre) decreases with time compared with Figure 6 time steps while flow in the spatially uncorrelated and the spatially strongly correlated poroperm structures (left and right) remains steadier.

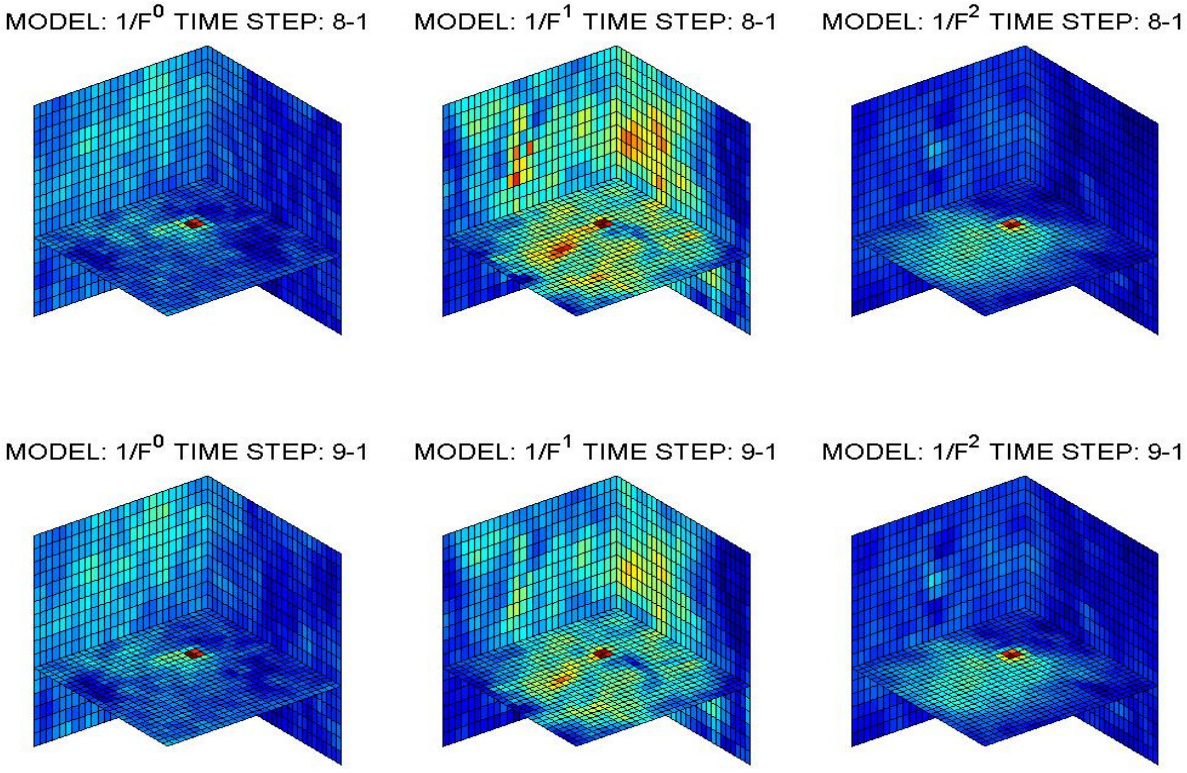

Figure 8: Snapshots for time-steps 8 and 9 of flow simulation described in Figure 5; flow in the 1/*f*-noise medium (centre) now increases with time compared with Figure 7 time steps as the pressure distribution readjusts in the complex flow structure; flow in the spatially uncorrelated and the spatially strongly correlated poroperm structures (left and right) diminish steadily.

Figures 5-8 illustrate the substantial dichotomy in flow regimes. Flow in (i) spatially uncorrelated permeability heterogeneity where average flow condition apply and/or (iii) strongly spatially correlated heterogeneity where flow concentrates in large-scale volumes offers the observer a chance of spatial simplicity. For the intermediate state of spatial complexity (ii), flow neither averages out material properties nor is smoothed by material property coherence over large volumes. Flow in heterogeneity types (i) and (iii) corresponds to general observer expectation of spatially tractable reservoir flow structures, while *in situ* flow in conforms to the more intractable heterogeneity type (ii), leading to persistent reservoir model failure.

Simulation pressure histories shown in Figures 9-12 reflect the distinct character of 1/*f*-noise heterogeneity flow evolution seen spatially in Figures 5-8. The four plots show time-evolving pressure signals recorded for a quartet observation wells proximate to one of four source wells. Each figure represents a different source well in the general vicinity of the source well shown in Figures 3-8.

The green traces of 1/*f*-noise heterogeneity are temporally irregular compared with blue traces of white noise heterogeneity red traces of Brownian noise heterogeneity. These pressure curves show that the different heterogeneity types result in substantially different interwell connectivity signals.

All pressure history curves evolve more or less consistently within their heterogeneity class. The uncorrelated heterogeneity (white noise, blue curves) and strongly correlated heterogeneity (Brownian noise, red curves) both have steady pressure evolution paths which bespeak their heterogeneity types. The blue curves of uncorrelated heterogeneity are relatively subdued in pressure history difference as expected from a medium that is essentially uniform within a standard deviation about the mean; there is no evidence of flow complexity associated with significant spatial trends in poroperm distribution. The red curves of Brownian-noise heterogeneity have a strong degree of temporal evolution that is the same for each source-sensor well pair so that evolution is spatially coherent throughout the large-scale spatially coherent poroperm structure visible in the right-hand column of Figures 5-8.

As noted for the spatial flow distributions, these results are understandable in terms of simple considerations: flow in spatially uncorrelated media conforms to the standard statistical expectation that randomness tends to average out and flow in strongly spatially correlated media tends to be coherent over the broad range of coherent spatial properties.

The green curves of 1/*f*-noise heterogeneity present a conceptually unfamiliar degree of flow complexity. The observed green-curve well pressure histories of Figures 9-12 respond to a spatially consistent but complex spatially-correlated heterogeneity structure, and the time evolution of the initial pressure signal is temporally complex. Compared with a typical well-pair history for the uncorrelated or strongly correlated poroperm heterogeneity classes, any given well-pair cross-correlation signal for 1/*f*-noise heterogeneity can be difficult to interpret. These pressure history simulations indicate how inherently complex *in situ* flow can be without invoking geologically-based heterogeneity.

The lesson held out by the Figure 9-12 pressure simulation data is that small spatial variations within a 1/*f*-noise heterogeneity structure can create strong ambiguities in well connectivity signal. It appears that understanding the spatial details of a 1/*f*-noise flow regime requires dedicated and extensive sampling of the reservoir pressure and flow history. Future flow simulation work can put bounds on the ability of a specific set of observational detail to resolve *in situ* flow regime and hence to more accurately guide the drill bit to productive high permeability reservoir volumes.

It is likely that purely well-data definition of geothermal reservoir flow structure can be usefully supplemented by fracture-sensitive geophysical field data (seismic velocity and EM sounding structure, microseismic activity, fracture alignment from shear-wave splitting and EM polarization data) interpreted in terms of the grain-scale fracture-density geophysics used here to define porosity and permeability structures. Such an exercise is described by Malin et al. (2009).

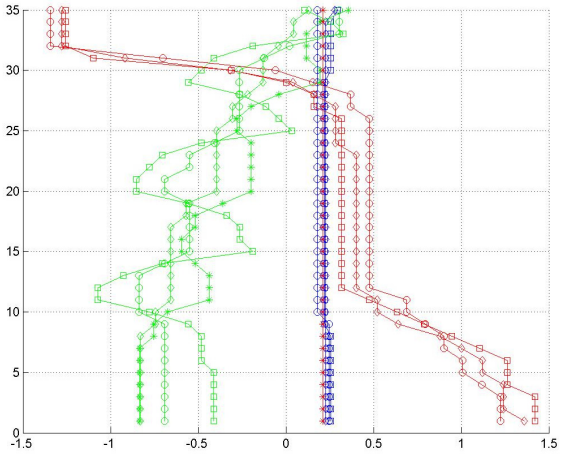

Figure 9: Pressure histories for four observation wells located at various offsets just above the plane of the simulation pressure source as shown in Figure 4. Blue, green and red curves denote data for, respectively, the spatially uncorrelated white-noise medium of Figure 1, the spatially correlated 1/*f*-noise medium of Figure 2, and the strongly spatially correlated Brownian noise medium of Figure 3.

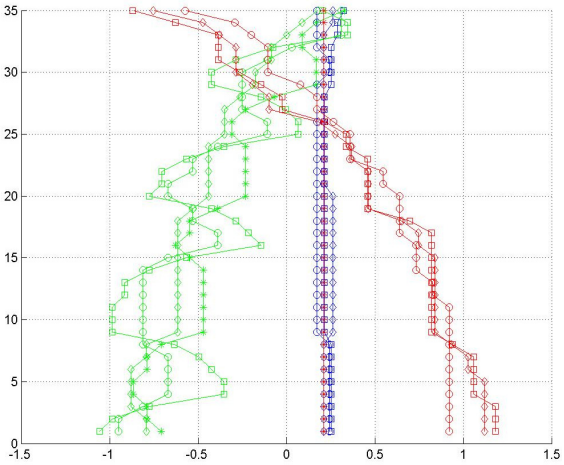

Figure 10: Pressure histories at four observation wells for three degrees of spatially correlated heterogeneity and different source point from Figure 9.

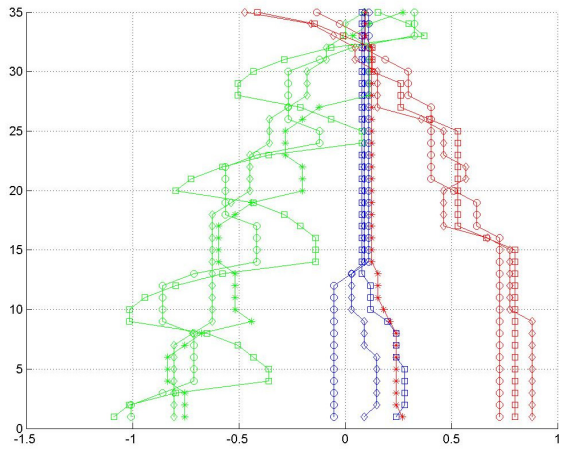

Figure 11: Pressure histories at four observation wells for three degrees of spatially correlated heterogeneity and different source point from Figures 9-10.

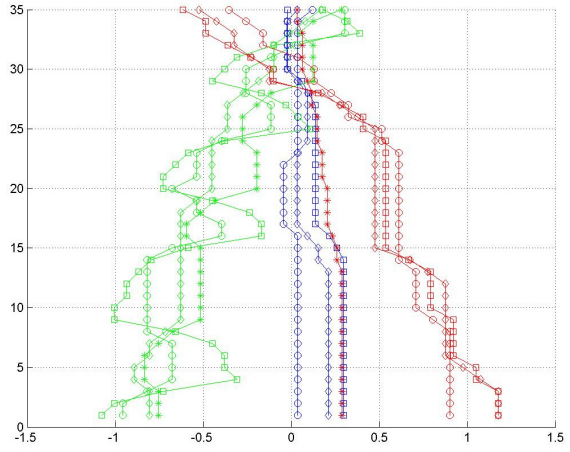

Figure 12: Pressure histories at four observation wells for three degrees of spatially correlated heterogeneity and different source point from Figures 9-11.

3. CONCLUSIONS

Simulations of Darcy flow are easily conducted by standard finite-element solvers for long-range spatially-correlated percolation-heterogeneous reservoir media as defined by *in situ* fracture systematics. The simulated percolation flow mechanics is directly based two well-attested features of *in situ* spatial fluctuations: (i) well-log geophysical measurement spatial correlation over many decades of scale length implies the existence of grain-scale fracture densities that control the fracture-nature of crustal rock and (ii) well-core poroperm fluctuations that physically link grain-scale density fluctuations to grain-scale percolation connectivity.

Geofluid flow in such media can be spatially and temporally simple if there is little long-range spatial correlation (white noise spatial heterogeneity) or strong spatial correlation (Brownian noise spatial heterogeneity). However, flow of geofluids is likely to be spatially and temporally complex for 1/*f*-noise heterogeneity characteristic of *in situ* crustal rock.

These flow simulation results imply that flow in real reservoirs can be dauntingly complex and admits of no simple modeling predictions. Understanding *in situ* reservoir flow requires systematic and extensive observation and interpretation of flow-related data such as the well-well connectivity simulated here, in all likelihood aided by supplemental geophysical field data systematically interpreted in terms of spatially fluctuating distributions of grain-scale fracture density that control *in situ* porosity and permeability.

REFRENCES

Horne, R.N., and Szucs, P.: Inferring well-to-well connectivity using nonparametric regression on well histories, Proceedings, Thirty-Second Workshop on Geothermal Reservoir Engineering, Stanford University, 22-24 January 2007

Horne, R.N.: Geothermal data mining – Value in antiques, Proceedings NZGW2008, Taupo, New Zealand, 11-13November 2008

Leary, P.C., 2002. In: JA Goff and K Holliger (Eds.): Heterogeneity of the Crust and Upper Mantle - Nature, Scaling and Seismic Properties, Kluwer/Academic/ Plenum Publishers, New York, 155-186

Leary, P.C., and Walter, L.A.: Crosswell seismic applications to highly heterogeneous tight gas reservoirs, First Break, 26, March 2008, 33-39

Leary, P.C., and Malin, P.E.: The Nature of Reservoir Fracture Heterogeneity: I - a New Conceptual and Computational Model, Paper 2237, Proceedings WGC2010, Bali, Indonesia, April 2010

Malin, P., Leary, P., Shalev, E., and Onacha, S.: 2009. Joint Geophysical Imaging of Poroperm Distributions in Fractured Reservoirs, Proceedings Geothermal Resources Council 2009 Conference and Exposition, Reno, NV, 4-7October 2009

Regenauer, K., Yuen, D.A., and Fuseis, F.: Landslides, icequakes, earthquakes: a thermodynamic approach to surface instabilities, Pure and Applied Geophysics 166, 1-24, (2009)

Turcotte, D.L.: Fractals and Chaos in Geology and Geophysics, Cambridge University Press, Cambridge, (1992)

Voss, C.I., and A.M. Provost: “SUTRA Version 2.1”, U.S. Geological Survey Water-Resources Investigations Report-02-4231, (2008), http://water.usgs.gov/nrp/ gwsoftware